

Stability of Coherently Strained Semiconductor Superlattices

R. G. Dandrea, J. E. Bernard, S.-H. Wei, and A. Zunger

Solar Energy Research Institute, Golden, Colorado 80401

(Received 11 September 1989)

The excess energy of several III-V and II-VI strained-layer semiconductor superlattices $(AC)_p(BC)_p$ is studied as a function of the repeat period p and orientation $\mathbf{G} = [001]$, $[110]$, $[111]$, and $[201]$, using **first-principles calculations**. We discover a number of universal features, including the predicted instability for nearly all p 's and \mathbf{G} 's with respect to *bulk* disproportionation, the identification of chalcopyrite as a metastable ordered structure, and the stability of all thin *epitaxial* $[110]$ and $[201]$ and most common-anion $[001]$ superlattices relative to coherent phase separation.

PACS numbers: 68.65.+g, 61.55.Hg, 68.60.Dv

Artificial growth of A_pB_p superlattices (SL's) is based on a series of *sequential exposures* of a substrate to pure compound A , then pure B , etc., thus largely circumventing the thermodynamically controlled *simultaneous* reaction $xA + (1-x)B \rightleftharpoons A_xB_{1-x}(\gamma)$, which could have otherwise produced a variety of microscopic arrangements γ ranging from disordered alloys to phase separation. Diffusion barriers¹ present in the SL make uncertain whether its apparent stability reflects these barriers or a genuine thermodynamic preference of $\gamma = \text{SL}$ over $\gamma = \text{disordered}$ or $\gamma = \text{phase separated}$. Postgrowth stability is addressed experimentally by reducing these kinetic barriers. Indeed, the introduction of fast-diffusing impurities¹ catalyzes the disordering of semiconductor SL's. Calculations²⁻⁵ for $p=1$ SL's have shown that the excess enthalpy is positive for isovalent SL's in the $[001]$ orientation, suggesting their thermodynamic instability. Yet, epitaxial growth appears to stabilize *spontaneously* ordered SL's, even without a free surface.^{6(a)} To clarify these issues, we use first-principles methods to investigate the excess enthalpy of the above reaction for a range of ternary III-V and II-VI semiconductor SL's as a function of repeat period p and orientation $\mathbf{G} = [001]$, $[110]$, $[111]$, and $[201]$, as well as for their 50%-50% disordered alloys. A number of universal features are discovered.

Since we are interested in low temperatures, we neglect entropy effects for the ordered SL's and phonon contributions to the *relative* energies of different structures. We distinguish three types of excess enthalpies. First, the *bulk* formation enthalpy $\Delta H(p, \mathbf{G})$ is the equilibrium SL energy minus that of equivalent amounts of the constituents at their *bulk* equilibria. Second, the *epitaxial* formation enthalpy $\delta H(a_s, p, \mathbf{G})$ is the energy of the SL, grown coherently on a substrate of lattice constant a_s , relative to the *epitaxial* constituents deformed to the same substrate a_s and relaxed in the perpendicular direction \mathbf{G} . Finally, the mixing enthalpy⁵ of the disordered (D) alloy $\Delta H^{(D)}(x, T)$ is the energy of the alloy at composition x and lattice constant $a(x)$ relative to equivalent amounts of the constituents at their bulk equilibria. Clearly, ΔH reflects the propensity for *incoherent bulk decomposition*, whereas δH measures the

propensity for decomposition into *coherently matched constituents*, appropriate to dislocation-free epitaxial systems. For substrates lattice matched to the equilibrium SL ($a_s = a_{\text{SL}}$), the difference $\Delta H - \delta H = \Delta E_{\text{CS}}$ is the "constituent strain" energy: the energy of the epitaxial constituents relative to their zinc-blende equilibria. For lattice-matched constituents, we expect $\Delta E_{\text{CS}} = 0$ and $\delta H = \Delta H$, while in lattice-mismatched systems studied here, $\Delta E_{\text{CS}} > 0$ and $\delta H < \Delta H$; hence bulk-unstable SL's can become epitaxially stable. In the $p \rightarrow \infty$ limit, the excess enthalpy ΔH (per 4 atoms) has but a negligible, $O(1/p)$, contribution from the interfaces, and thus approaches the constituent strain energy:

$$\Delta H(p, \mathbf{G}) = \frac{2I(p, \mathbf{G})}{p} + \Delta E_{\text{CS}}(a_{\text{SL}}, \mathbf{G}). \quad (1)$$

Here $I(p, \mathbf{G})$ is the interfacial energy (independent of p for large p), and is simply related to the epitaxial energy $\delta H = \Delta H - \Delta E_{\text{CS}} = 2I/p$.

All $T=0$ energies were calculated self-consistently in the local-density approximation. We have used both the general-potential linear-augmented-plane-wave⁷ (LAPW) method, and the nonlocal pseudopotential⁸ plane-wave method,⁹ with a 15-Ry cutoff. Structural parameters were obtained from first principles for $p=1$ $[001]$ LAPW calculations and for all pseudopotential calculations (the cell internal parameters being determined by iteratively relaxing calculated Hellmann-Feynman forces^{9,10}). The SL lattice constant was found to be the average of the binaries. These calculations found good agreement with determinations using a purely elastic valence-force-field¹¹ (VFF) model, and so this model was used to determine nuclear positions in the remaining LAPW studies. As for the disordered alloy, the mixing enthalpy $\Delta H^{(D)}$ was obtained by solving the fcc Ising Hamiltonian, using up to four-body and fourth-fcc-neighbor interaction energies extracted from a cluster expansion of the energies of eight short-period SL's.⁵ We estimate an overall uncertainty of 2 meV/atom in ΔH , due largely to small errors in calculated lattice constants (1%-2%) and bulk moduli (3%-7%) affecting ΔE_{CS} .

Table I¹²⁻¹⁴ gives $\Delta H(p, \mathbf{G})$ including $\Delta H(\infty, \mathbf{G})$

TABLE I. Formation enthalpy $\Delta H(p, \mathbf{G})$, interfacial energy $I(p, \mathbf{G})$, and mixing enthalpy of the disordered alloy $\Delta H^{(D)}$ ($x = \frac{1}{2}$, $T = 800$ K), in meV/(4 atoms). The heading lists the smaller binary first, and gives the electronegativities (Ref. 12) χ of the noncommon atoms. Sets of \mathbf{k} points equivalent (Ref. 13) to two [for LAPW (Ref. 14)] or ten (for pseudopotential) special zinc-blende \mathbf{k} points were used. All tabulated results are LAPW, except Ga₂PAs (pseudopotential). Pseudopotential calculations used the Ceperley-Alder exchange-correlation potential; LAPW used the same for Ga₂AsSb and GaInAs₂, and Hedin-Lundqvist for the rest. Pseudopotential results not tabulated are as follows: for Ga₂PAs, $\Delta H(3, [110]) = 19.8$, $\Delta H(2, [111]) = 36.9$, $\Delta H(3, [111]) = 36.4$; for AlInP₂, $\Delta H(1, [001]) = 43$, $\Delta H(1, [111]) = 97$; for Ga₂AsSb, $\delta H(1, [001]) = 33$, $\Delta H(1, [001]) = 121$; for AlInAs₂, $\Delta H(1, [001]) = 35$. Other LAPW: for AlInP₂, $\delta H(1, [001]) = -51$, $\Delta H(1, [001]) = 45$; for In₂PAs, $\Delta H(1, [001]) = 19$.

χ	GaAs	GaP	GaP	GaAs	ZnTe	ZnTe
	GaSb	GaAs	InP	InAs	HgTe	CdTe
	1.9	2.0	1.7	1.7	1.9	1.7
[001]						
$\Delta H(1)$	115	26.6	91	66.7	42.5	54.2
$\Delta H(2)$	97	24.3	95	62.4	46.5	59.4
$\Delta H(3)$	93	23.2				
$\Delta H(\infty)$	80	20.2	98	72.1	60.0	64.8
$I(2)$	17	4.1	-3	-9.7	-13.5	-5.4
[110]						
$\Delta H(1)$	115	26.6	91	66.7	42.5	54.2
$\Delta H(2)$	80	18.1	73	47.3	49.1	56.1
$\Delta H(\infty)$	105	28.3	135	94.8	95.8	97.2
$I(2)$	-25	-10.2	-62	-47.5	-46.7	-41.1
[111]						
$\Delta H(1)$	132	37.2	155	108.5	103.3	103.5
$\Delta H(\infty)$	109	36.3	147	100.2	101.6	103.1
$I(1)$	11.5	0.5	3.5	4.1	0.9	0.2
[201]						
$\Delta H(1)$	115	26.6	91	66.7	42.5	54.2
$\Delta H(2)$	52	6.5	19	16.5	11.4	19.2
$\Delta H(\infty)$	97.7	27.5	125	87.0	75.6	76.3
$I(2)$	-45.7	-21.1	-106	-70.5	-64.2	-57.1
Alloy						
$\Delta H^{(D)}$	86	18.7	66.6	51.0	40.8	49.7

$= \Delta E_{CS}$, $I(p, \mathbf{G})$, and $\Delta H^{(D)}$. Figure 1(a) shows results for a representative case. Past calculations of $\Delta H(p, \mathbf{G})$ of strained-layer SL's are mostly limited to one geometry: $p=1$ and $\mathbf{G}=[001]$. Reference 3 finds $\Delta H = 129.2$, 115.6, and 83.6 meV/(4 atoms) for Ga₂AsSb, GaInP₂, and GaInAs₂, respectively; Reference 4 finds 114.8 for Ga₂AsSb and Ref. 2 finds 60.1 for GaInAs₂. Our results agree closely with those of Refs. 2 and 4, but disagree by up to 25 meV/(4 atoms) with those of Ref. 3. The present calculations, however, used larger basis

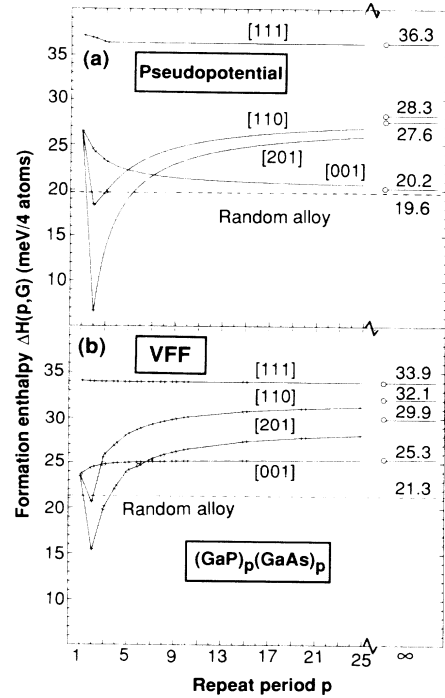


FIG. 1. Formation enthalpy of $(\text{GaP})_p(\text{GaAs})_p$ vs repeat period p and orientation \mathbf{G} . (a) First-principles pseudopotential calculations. (b) VFF calculations. The strain energies of the epitaxially deformed binaries ($p = \infty$) are shown at the right.

sets and full structural relaxation. Our basic conclusions are as follows.

(i) In the $p \rightarrow \infty$ limit we find the universal order

$$\Delta H([001]) < \Delta H([201]) < \Delta H([110]) < \Delta H([111]); \quad (2)$$

hence the conventional [001] growth direction is indeed the stablest for *long-period* SL's. This can be understood from harmonic elasticity theory, where the energy density U of a coherently strained film is written as a quadratic form in the strains ϵ_{\parallel} and ϵ_{\perp} parallel and perpendicular to the substrate. The condition $dU/d\epsilon_{\perp} = 0$ for fixed ϵ_{\parallel} gives the strain energy per fcc site as¹⁵

$$E(a_s, \mathbf{G}) - E_{eq} = \frac{9}{8} q(\mathbf{G}) B a_{eq} (a_s - a_{eq})^2, \quad (3)$$

where E_{eq} is the energy of the unstrained film, $B = (C_{11} + 2C_{12})/3$ is the bulk modulus, C_{ij} are elastic constants, and all orientation dependence lies in the epitaxial-strain-reduction factor¹⁵ $q(\mathbf{G}) = 1 - B/[C_{11} + \gamma(\mathbf{G})\Delta] < 1$ (for isotropic compression $q=1$). Here $\Delta = C_{44} - (C_{11} - C_{12})/2$ is the elastic anisotropy, $\gamma([001]) = 0$, $\gamma([201]) = \frac{16}{25}$, $\gamma([110]) = 1$, and $\gamma([111]) = \frac{4}{3}$. As ΔE_{CS} is simply the sum of Eq. (3) over both binaries, the fact that tabulated elastic constants¹⁶ show $\Delta > 0$ for all diamondlike, III-V and II-VI zinc-blende semiconductors means the order of Eq. (2) simply reflects the order of the geometric factors $\gamma(\mathbf{G})$. The

lead chalcogenides and all the alkali halides except the Li salts have¹⁶ $\Delta < 0$; for them the order of $\Delta H(\infty, \mathbf{G})$ is thus exactly reversed relative to Eq. (2).

(ii) For short-period SL's, the stability sequence differs (Fig. 1) from that of Eq. (2), reflecting interfacial effects rather than the constituent's strain. To analyze this it is useful to think of $I(p, \mathbf{G})$ as having a classical "strain-relief" piece I_{SR} due to atomic relaxation near the interface and a "charge-exchange" piece I_{CE} due to interfacial electronic charge redistributions. To isolate the first contribution we have calculated $\Delta H(p, \mathbf{G})$ using the *purely elastic* VFF model.¹¹ The results for GaP-GaAs [Fig. 1(b)] illustrate that for $\mathbf{G}=[001]$ and $[111]$ $\Delta H(p)$ is nearly constant, and hence $I_{SR} \approx 0$, while for $\mathbf{G}=[110]$ and $[201]$ $\Delta H(p)$ for small p is well below the $p = \infty$ values, and so $I_{SR} \ll 0$. This reflects large energy-lowering relaxations of interfacial atoms for these latter orientations (for $p \geq 2$; for $p=1$, the $[001]$, $[110]$, and $[201]$ SL's are identical), and leads universally to the $p=2$ $[201]$ SL's (chalcopyrites) having the lowest SL energy. These large relaxations are demonstrated in Fig. 2, depicting the interlayer spacings in the $p=15$ $[110]$ SL; the relaxations in the $[001]$ and $[111]$ SL's (not shown) are negligible on the scale of Fig. 2. The absence of large interfacial atomic relaxations for the $[001]$ and $[111]$ SL's reflects the high symmetry of the interfacial atoms in those cases: For $[001]$ and $[111]$ the interfacial atoms are surrounded by only two types of bonds arranged symmetrically about the interface, while for $[110]$ and $[201]$ three and four (respectively) inequivalent bonds surround an interfacial atom, and the resulting asymmetry drives large relaxations.

(iii) As the $[001]$ interfacial energy is controlled by I_{CE} , it is natural to inspect the self-consistent charge rearrangement in these systems relative to their epitaxially deformed binaries. Figure 3 (and similar constructs for other systems) shows that *overall* charge is always transferred from the constituent with the smaller to that with the larger lattice constant. We find that whether

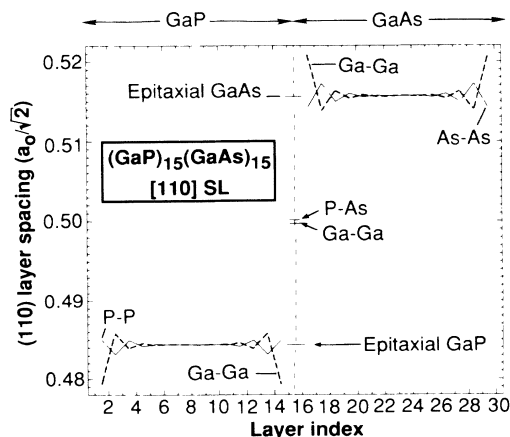


FIG. 2. Interlayer spacing for the $(\text{GaP})_{15}(\text{GaAs})_{15}$ $[110]$ SL, as determined by the VFF model.

this direction of size-mismatch-induced charge transfer is stabilizing ($I < 0$) or destabilizing ($I > 0$) depends on whether it also coincides with the direction mandated by electronegativities: Transfer to a more (less) electronegative region leads to $I < 0$ ($I > 0$). From Table I it is seen that our results, in general,¹⁴ follow the "interfacial energy rule" for lattice-mismatched systems, stating that " $I([001])$ is negative (positive) if the smaller of the two constituents has a smaller (larger) electronegativity." It is also seen that the common-anion SL's generally have $I([001]) < 0$, whereas the common-cation SL's have $I([001]) > 0$. This can be related to the above rule by noticing that electronegativities¹² increase going *up* columns VB-VIIB, but increase going *down* columns IIB and IIIB (neglecting boron) of the periodic table, whereas sizes increase going *down* all these columns [the two exceptions of Al-Ga and Cd-Hg leading to lattice-matched AlGaAs and HgCdTe SL's that, although being common-anion, have⁵ $I([001]) > 0$]. The physical origins of this behavior are reflected in atomic-valence-orbital energies, which generally become more negative going *up* a column, but which often deviate from that behavior in the cation columns IB-IIIB (where the delocalized outer d orbitals screen the nuclear charge less well than does the tighter d shell in the VB-VIIB anions).

To test these ideas we calculated $\delta H(1, [001])$ for AlX-InX , with $X=\text{P}$ or As . The rule predicts a negative interfacial energy ($\chi_{\text{Al}}=1.5$, $\chi_{\text{In}}=1.7$), and we indeed find $\delta H = -35$ and -33 meV/(4 atoms) for $X=\text{P}$ and As , respectively. The large negative δH 's for AlX-InX ,

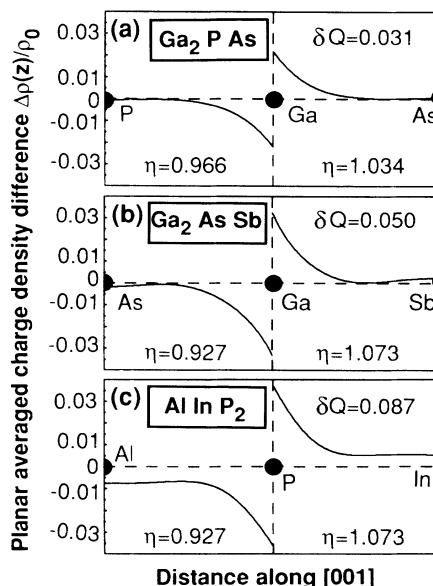


FIG. 3. Charge-density differences (SL minus epitaxial binary, averaged in planes orthogonal to $[001]$) for three $p=1$ $[001]$ SL's, in units of the mean SL valence charge density ρ_0 . $\eta = c/a_z$ is the tetragonal distortion in each half of the SL, and δQ is the number of electrons (per SL unit cell) transferred between the two halves.

contrasted with the near vanishing¹⁴ values for GaX-InX, can be understood using pseudopotential total energies in place of the atomic electronegativities above: The GaX-InX binaries are nearly degenerate [$E(\text{InX}) - E(\text{GaX}) \approx -0.03 \text{ Ry}$], while $E(\text{InX}) - E(\text{AlX}) \approx -1.28 \text{ Ry}$ is 40 times more negative (X dependences here are less than 0.02 Ry). Also, note that these four systems (AlX-InX and GaX-InX) demonstrate the near X dependence of δH , as implied by the interfacial energy rule. Finally, note that for [111] the favorable I_{CE} effects of common-anion systems do not manifest themselves so simply as for [001]: δH is small and positive for all [111] systems in Table I. However, for AlP-InP we do find $\delta H(1, [111]) = -19 \text{ meV}/(4 \text{ atoms})$.

(iv) For all systems in Table I, we find that the interfacial energy terms $2I/p = \delta H$ are smaller in magnitude than the (positive) constituent strain energies, so that $\Delta H(p, \mathbf{G}) > 0$. This means that under bulk equilibrium conditions, all these systems will prefer phase separation to SL ordering. However, items (ii) and (iii) above suggest that it might be possible to combine the favorable strain-relief characteristics of the $p=2$ [201] interfaces with the favorable charge-exchange chemistry of common-anion systems to lead to an *overall negative* formation enthalpy even in bulk form ($\Delta H < 0$). We have thus studied the $p=2$ [201] AlInX_2 systems, and find $\Delta H = -21$ and $-15 \text{ meV}/(4 \text{ atoms})$ for $X=\text{P}$ and As , respectively; these chalcopyrite structures are thus predicted to be stable even towards *bulk* phase separation.

(v) Table I gives the mixing enthalpies of the $x = \frac{1}{2}$ disordered alloy as calculated by the cluster-variation method.⁵ It shows that [001] and [111] SL's are of higher energy than the disordered alloy; these systems are thus predicted to be unstable *both* with respect to phase separation ($\Delta H > 0$) and with respect to disordering ($\Delta H > \Delta H^{(D)}$). On the other hand, the $p=2$ [201] SL's are always of lower energy than the disordered alloy: For all but AlInX_2 (which is *absolutely* stable), they are truly *metastable*, in the sense that they are unstable only with respect to phase separation but are stable (below a critical temperature) with respect to disordering. This is consistent with the [201] ordering observed recently in $\text{In}_{0.5}\text{Ga}_{0.5}\text{As}$ ^{6(a)} and $\text{GaAs}_{0.5}\text{Sb}_{0.5}$.^{6(b)}

In summary, starting from equilibrium constituents, epitaxial deformation raises their energy in proportion to the values of $q(\mathbf{G})$, making the long-period [001] system of lowest energy and the [111] of highest. Creation of A - B interfaces produces an interfacial energy which is dominated by a (usually) small charge-exchange component for $\mathbf{G}=[001]$ and [111], and by a large negative

strain-relief component for $\mathbf{G}=[110]$ and [201]. The latter effect lowers the energy of the short-period [110] and [201] SL's below that of [001] and yields universally $\delta H(p, \mathbf{G}) < 0$ for $\mathbf{G}=[110]$ and [201], while for $\mathbf{G}=[001]$ a favorable charge exchange leads to $\delta H < 0$ for most common-anion systems. Such systems with $\delta H < 0$ would not phase separate if grown in films sufficiently thin.¹⁵ Chalcopyrite always has lower energy than the disordered alloy at $x = \frac{1}{2}$; for AlInP_2 and AlInAs_2 it is also stabler than the phase separated system, while for other cases it is at least metastable. No other orientation produces bulk stability or (consistently) metastability.

This work was supported by the U.S. Department of Energy, Office of Energy Research, Basic Energy Science, Grant No. DE-AC02-77-CH00178.

¹W. D. Laidig, N. Holonyak, M. D. Camras, K. Hess, J. J. Coleman, P. D. Daphys, and J. Bardeen, Appl. Phys. Lett. **38**, 776 (1981).

²T. Ohno, Phys. Rev. B **38**, 13 191 (1988).

³P. Boguslawski and A. Baldereschi, Solid State Commun. **66**, 679 (1988); Phys. Rev. B **39**, 8055 (1989).

⁴A. Qteish, N. Motta, and A. Balzarotti, Phys. Rev. B **39**, 5987 (1989).

⁵L. G. Ferreira, S. H. Wei, and A. Zunger, Phys. Rev. B **40**, 3197 (1989).

⁶(a) H. Nakayama and H. Fujita, in *GaAs and Related Compounds—1985*, edited by F. Fujimoto, IOP Conference Proceedings Series No. 79 (Adam Hilger, Bristol, 1986), p. 289; (b) H. R. Jen, M. J. Cherng, and G. B. Stringfellow, Appl. Phys. Lett. **48**, 1603 (1986).

⁷S. H. Wei and H. Krakauer, Phys. Rev. Lett. **55**, 1200 (1985).

⁸G. Kerker, J. Phys. C **13**, L189 (1980).

⁹J. Ihm, A. Zunger, and M. L. Cohen, J. Phys. C **12**, 4409 (1979).

¹⁰O. H. Nielsen and R. M. Martin, Phys. Rev. B **32**, 3780 (1985).

¹¹P. N. Keating, Phys. Rev. **145**, B637 (1966).

¹²L. Pauling, *The Nature of the Chemical Bond* (Cornell Univ. Press, Ithaca, 1960), 3rd ed., p. 93.

¹³S. Froyen, Phys. Rev. B **39**, 3168 (1989).

¹⁴At two (ten) \mathbf{k} points, LAPW calculations give [in meV/(4 atoms)] $\delta H(1, [001]) = -7$ (-1) for GaP-InP, and $\delta H(1, [001]) = -5.4$ ($+1.3$), $\delta H(2, [001]) = -9.7$ ($+0.8$) for GaAs-InAs.

¹⁵D. M. Wood and A. Zunger, Phys. Rev. B **40**, 4062 (1989).

¹⁶G. Simmons and H. Wang, *Single Crystal Elastic Constants* (MIT Press, Cambridge, 1978).